Process Optimization for Catalytic Oxidation of Dibenzothiophene over UiO-66-NH2 by Using Response Surface Methodology

Journal:	*ACS Omega*
Manuscript ID	ao-2021-05965c
Manuscript Type:	Article
Date Submitted by the Author:	25-Oct-2021
Complete List of Authors:	Barghi, Bijan; Virumaa College Of Tallinn University Of Technology, School of Engineering Jürisoo, Martin ; Virumaa College Of Tallinn University Of Technology, School of Engineering Volokhova, Maria; National Institute of Chemical Physics and Biophysics Seinberg, Liis; National Institute of Chemical Physics and Biophysics Reile, Indrek; National Institute of Chemical Physics and Biophysics, Mikli, Valdek; Tallinn Technical University, Department of Chemistry and Materials Technology Niidu, Allan; Virumaa College Of Tallinn University Of Technology, School of Engineering

Process Optimization for Catalytic Oxidation of Dibenzothiophene over UiO-66-NH_2 by Using Response Surface Methodology

Bijan Barghi[a1], *Martin Jürisoo*[a], *Maria Volokhova*[b], *Liis Seinberg*[b], *Indrek Reile*[b], *Valdek Mikli*[c], *Allan Niidu*[a]

a) Virumaa College, School of Engineering, Tallinn University of Technology, Järveküla tee 75, 30322 Kohtla-Järve, Ida-Viru maakond, Estonia

b) National Institute of Chemical Physics and Biophysics, Akadeemia tee 23, 12618, Tallinn, Estonia

c) Department of Chemistry and Materials Technology, School of Engineering, Tallinn University of Technology, Ehitajate tee 5, 19086, Tallinn, Estonia

*Corresponding author, bibarg@taltech.ee

Oxidative Desulfurization, Dibenzothiophene, Metal Organic Framework, Characterization, Response Surface Methodology

This research investigates the catalytic performance of a ligand modified metal organic framework (MOF) prepared by a solvothermal method for oxidative desulfurization of dibenzothiophene (DBT) in n-dodecane as a fuel model (FM). The prepared catalyst was characterized by several methods including XRD, FTIR, H NMR, SEM, TGA and MP-AES analysis. A response surface methodology with the principles of central composite design (CCD) was employed for the optimization process and design of experiments. The effects of reaction conditions including temperature (X_1), oxidant over sulfur (O/S) mass ratio (X_2), and catalyst over sulfur (C/S) mass ratio (X_3) were assessed on DBT removal efficiency. Accordingly, optimal operation conditions for sulfur removal were obtained when the temperature, O/S mass ratio, and C/S mass ratio were 72.6 ℃, 1.62 (mg/mg) and 12.1 (mg/mg) respectively. Moreover, a DBT removal of 94% was attained for FM using MOF as the catalyst in optimal reaction

conditions. In this quadratic model, F-values showed 20.16, which gave evidence that the model was well-fitted.

1. Introduction

Nowadays, most countries which implemented strict regulations for fossil fuels in favor of environmental protection have prompted an increasing interest in research to improve deep desulfurization technologies [1-3]. Hydrodesulfurization (HDS) is one of the efficient methods in removing sulfurs [4-5]; however, it is less pivotal for planar sulfur-containing compounds, such as benzothiophene and dibenzothiophene. It requires severe operating conditions, including high H2 pressure and temperature as well as larger reactors and highly active catalysts [6-7]. Hence, alternative approaches were required to achieved deep desulfurization to produce clean transportation fuels such as selective adsorption, alkylation desulfurization, biodesulfurization, and oxidative desulfurization (ODS). ODS is a green and promising process for deep desulfurization that can be conducted under ambient operation conditions, and it prevents the use of hydrogen. In ODS systems, the sulfur-removal efficiency of catalysts is increased when S-compounds are oxidized [8-11].

Employing an appropriate catalyst improves the activity of oxidants in the ODS process. Metal Organic Frameworks (MOFs) are candidates that contain the rigidity of inorganic secondary building units (SBUs) with the flexibility and tunability of organic linkers [12-15]. Among the hybrid MOFs, UiO-66(Zr) derivates are impressively contributing to both scientific and industrial applications. It was reported that pristine UiO-66 could achieve over 90% ODS removal in a short reaction time [16-19], moreover, other functional groups (-NH_2, -OH) could also significantly affect its chemical activity and it is reported that they provide a strong affinity for sulfur oxidation [19-22]. Presently, in some cases, UiO-66-NH_2 has been applied for desulfurization reaction [23-25], even though there is no investigation on statistical optimization of the MOF amount.

There are various oxidant agents such as hydrogen peroxide, oxygen, and tertbutyl hydroperoxide have been reported in the preceding studies. However, hydrogen peroxide has been used as the more promising oxidant due to its commercial availability, high selectivity, and environmental issues [26-29].

In this study, amin functional group (–NH_2) was used to synthesize functionalized UiO-66(Zr) by solvothermal method as the catalyst for ODS reaction. The characterization of prepared samples

was performed in detail via various techniques. The impact of reaction conditions and the performance of UiO-66-NH_2 in DBT oxidative removal were systematically investigated leading to optimal operational conditions. To understand the importance of parameters, temperature, oxidant amount, and catalyst dosage a quadratic statistical model was developed, and optimal conditions were derived by employing response surface methodology (RSM).

2. Experimental

2.1. Synthesis of UiO-66-NH_2

UiO-66-NH_2 was prepared as reported [30]. Briefly, 1 g of ZrCl4 and 1.07 g 2-amino terephthalic acid (NH_2-BDC) were dissolved in 120 ml N,N-dimethylformamide (DMF) and 8 ml concentrated HCl with sonication for 30 minutes. The produced solution was placed in an oven at 80 ˚C for 24 h. After naturally cooling to room temperature, the product was washed three times with DMF and three times with ethanol to remove all residual solvent. Then the sample was activated by heating to 80 ˚C under vacuum until a pressure of 600 mbar was reached. The synthesis procedure was depicted in Figure 1.

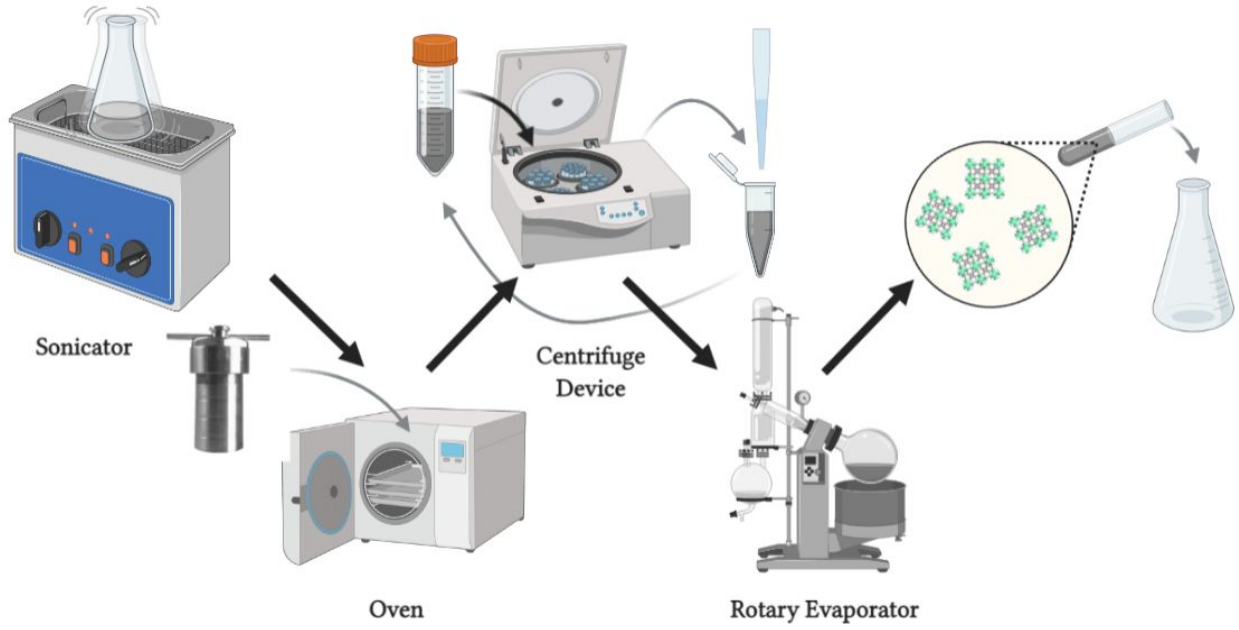

Fig. 1. Schematic of the solvothermal synthesis of UiO-66-NH_2

2.2. Characterization methods:

X-ray powder diffraction (XRD) patterns were measured by a Rigaku, Ultima IV or Panalytical XPert3 powder and a 1D strip detector for the range of $2^\circ < 2\theta < 45^\circ$. The functional moieties of the samples were characterized by a Fourier transform infrared spectroscopy (Thermo Scientific Nicolet iS50 FTIR Spectrometric Analyzer) in the range of 400–4000 cm^{-1} wavelength. Scanning electron microscopy (SEM) images were obtained on a Zeiss FEG-SEM Ultra-55 as well surface elemental composition of selected materials using EDS. The thermal stability of materials was tested by a simultaneous thermal analyzer (Mettler-Toledo TGA 1) temperature range from 10 ˚C to 800 ˚C and at heating rate 10 ˚C min^{-1}. Microwave plasma atomic emission

spectroscopy (MP-AES) was used to determine the purity of a sample as well as elemental ratios, on an Agilent 4200 Microwave Plasma Atomic Emission Spectrometer. Proton NMR spectrometry for digested MOF samples was carried out on an Agilent DD2 500 MHz (11.7T/51 mm) with 5 mm X{1H} DB PFG probe head (X = 15N…31P) for solution NMR experiments in the temperature region -80-130 ˚C. NMR analysis was used to determine the bulk purity of a MOF by digesting 1-2 mg of sample in 5-10 drops NaOD / D_2O solution and sonicating the mixture until the sample was well dispersed in the acid.

2.3. Oxidative desulfurization process

Catalytic Oxidation of DBT was carried out in an 8-dram glass batch reactor equipped with a thermometer, magnetic stirrer, and an oil bath for temperature control. In a typical run, 6 ml acetonitrile (aqueous phase) and 6 mL of a solution of DBT in n-dodecane (fuel phase) with 1000 ppm sulfur concentration were added to the reactor with the desired amount of MOF as the catalyst. The reactor was heated up to a specified temperature (20-100 ℃), then the determined amount of H_2O_2 was added at atmospheric (1 bar) pressure. The solution was vigorously stirred (600 rpm) to minimize the resistance of mass transfer. The effect of three main factors including reaction temperature, the initial mass ratio of oxidant to the total initial amount of sulfur, and

catalyst dosage was investigated. Upon completion of the reaction (150 minutes), the oil phase was taken for analysis of DBT oxidation. The samples were finally analyzed by a gas chromatograph mass spectrometer Shimadzu QP2010 plus. The removal efficiency of sample sulfur compounds obtained from the experiments was calculated as follows Equation (1):

$$Sulfur\ Removal\ (\%) = (S_0 - S_t)/S_0 \quad (1)$$

Where S_0 is the initial concentration of sulfur in FM and S_t is the sulfur concentration of the treated FM after ODS reaction time (t).

2.4. Statistical analysis method

To investigate the effect of specific factors on an output response, a central composite design (CCD) with a quadratic model was employed [31]. In this method, independent variables are coded at five levels: the central point is represented by 0; -1 and +1 coded levels represent factorial points; finally, $+\alpha$ and $-\alpha$ are known as axial points. Analysis of variance (ANOVA) was used for analyzing the data factors and main effects and their interactions of the process factors and responses were estimated [32]. The experimental coded levels and range of factors have been demonstrated in Table 1. The mathematical relationship of the response on the X_1, X_2, and X_3 parameters is given by the quadratic equation model as follows in Equation (2):

$$Y = \beta_0 + \sum_{i=1}^{3} \beta_i X_i + \sum_{i=1}^{3} \sum_{j=1}^{3} \beta_{ij} X_i X_j + \varepsilon \quad (2)$$

Where X_i and X_j are variables, Y represents the predicted response, β_0 is a constant term, β_i the coefficient of the linear terms, β_{ij} the coefficient of interaction terms and, ε is residual related to the experiments. The experiments (N) are determined by the following Equation (3):

$$N = 2^k + 2 * k + n_0 \quad (3)$$

Where k is the number of independent parameters; 2^k is the number of experiments for the variables having the code value equal to ±1 (factorial points); $2 * k$ is the number of experiments for the variables with the code value equal to $\pm\ \alpha$ (axial points), and n_0 is the number of experiments for the variables having a code value equal to 0 (central point). Based on CCD method, a total, 17 test runs were performed for ODS reaction optimization.

Table 1: Independent test variables at five levels used for central composite design

Factor	Unit	Code	Real Values of Coded Levels				
			Low Axial (-α*)	Low Factorial (-1)	Center Point (0)	High Factorial (+1)	High Axial (+α*)
Temperature	°C	X_1	20	36.21	60	83.78	100

O/S ratio	-	X_2	0.5	1.61	3.25	4.89	6
C/S ratio	-	X_3	0.5	3.44	7.75	12.06	15

*α: 1.68

Standard uncertainties (u) are u(T) = ± 0.1 °C; u(O/S ratio) = ± 0.01; u(C/S ratio) = ± 0.01

The coefficient of determination (R^2) was used for evaluating the accuracy of the quadratic model. Also, the terms of the proposed model were investigated by the determination of probability value (p-value) with a 95% confidence level. Moreover, for obtaining the highest removal factors, highest desirability, and statistical techniques. The arrangement of CCD, statistical studies, and optimizing processes was conducted using Design-Expert version 12 software.

3. Results and discussion

3.1. Characterization

As illustrated in Figure 2a, XRD was used to evaluate the structure and crystallinity of UiO-66-NH_2. The diffraction of this sample depicted the XRD patterns of the as-synthesized UiO-66-NH_2 which is identical to the reported XRD patterns and confirmed the UiO-66-NH_2 have been successfully prepared [33-34].

The FT-IR spectrum of the sample was presented in Figure 2b. For UiO-66-NH_2, the spectral band positioned at 1658 cm^{-1} was attributed to the stretching vibrations of C=O in the carboxylic

acid, indicating that DMF resides in the pores. Besides, the IR bands due to the O–C–O asymmetric (at 1571 cm^{-1}) and symmetric stretching of terephthalic acid ligand (1387 cm^{-1}) were visible, respectively. Meanwhile, the IR bands at 1491 cm^{-1} assigned to the vibration of C=C bonds of aromatic rings, while the IR peaks centered at 766 and 662 cm^{-1} were probably associated with –OH and C–H vibrations in the H_2BDC ligand. The peak at 1438 cm^{-1} can be attributed to the N–H bending vibration and C–N stretching vibration [35-36]. Also, UiO-66(Zr)-NH_2 displayed one small absorption peak at 3631 cm^{-1}, this peak was ascribed to the asymmetrical and symmetrical stretching vibration adsorption of the $–NH_2$ group [37].

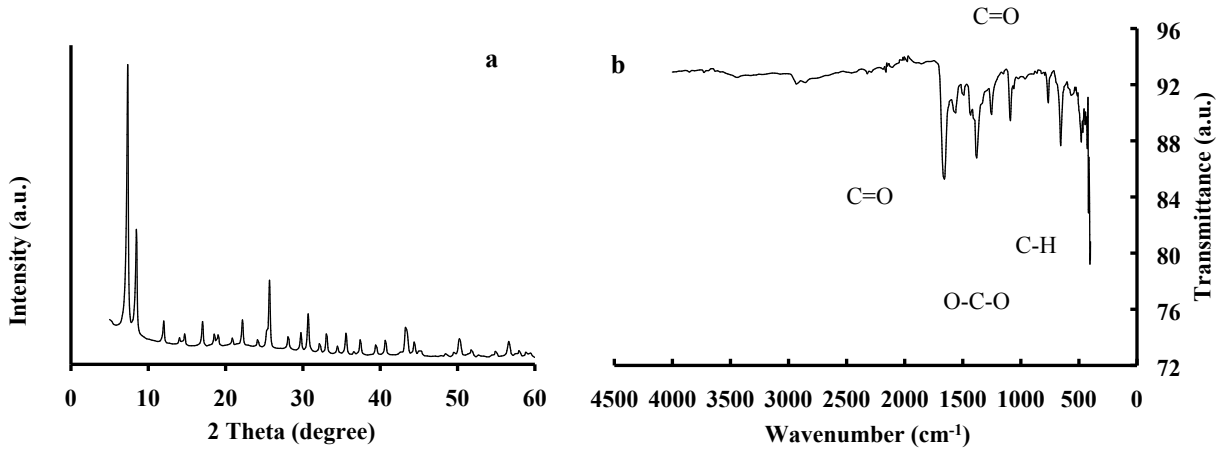

Fig. 2 XRD patterns (a) and FT-IR spectra (b) of UiO-66-NH_2

From the SEM picture (Figure 3), the UiO-66-NH2 samples exhibited uniform octagonal morphology. Based on the images, the particle sizes generally converged around 260 nm.

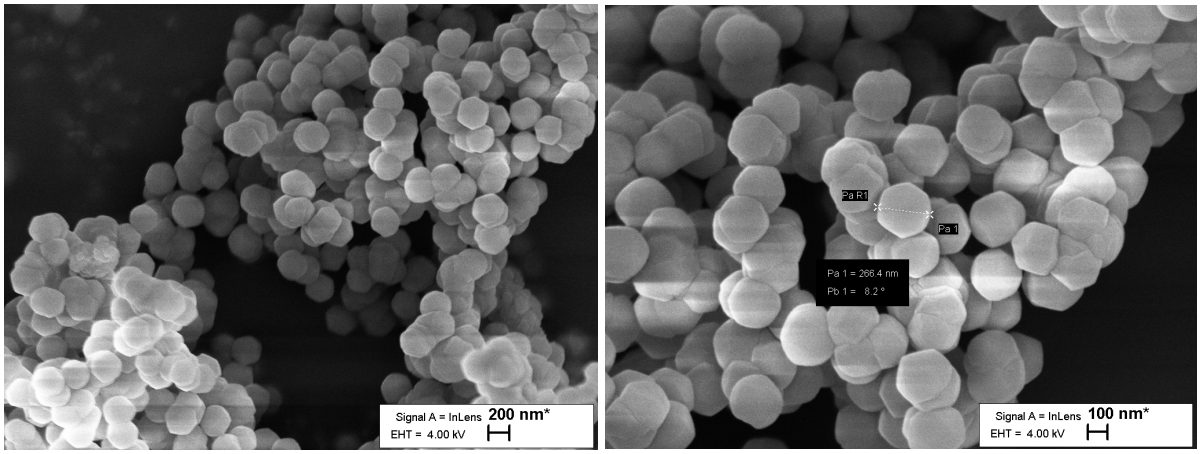

Fig. 3 Typical SEM images UiO-66-NH_2

Figure 4 showed the ^1H NMR spectra of solvothermal synthesized UiO-66-NH_2 after digestion in NaOD / D_2O solution. In UiO-66-NH_2, the three proton signals of 6.84, 6.90 and 7.35 ppm were attributed to the benzene ring structure of amino terephthalic acid in MOF [38].

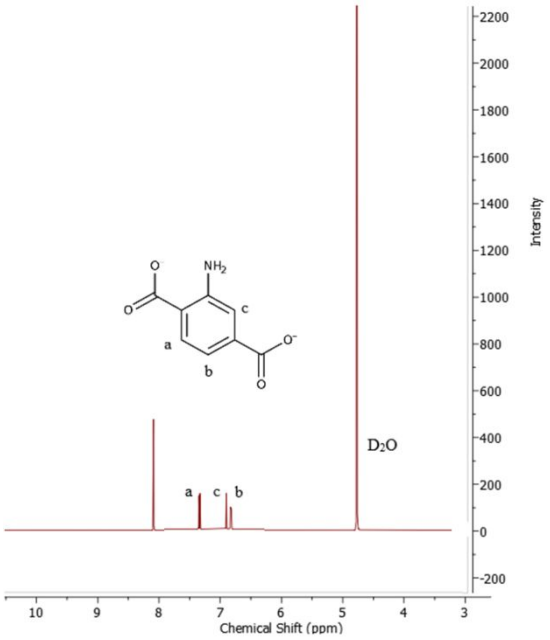

Fig 4. ^{1}H NMR spectra of UiO-66-NH_2 solution of NaOD / D_2O before NMR measurement.

The TGA curves of UiO-66-NH_2 was shown in Figure 5. The TGA curves of UiO-66-NH_2 showed a three-step weight loss. The initial mass loss at 45–130 °C was assigned to the removal of ethanol and water remained solvent and the second mass loss was for DMF removal coordinated with Zr-O. The third step weight loss after 500 °C was due to residual solvent molecule`s dehydroxylation of the zirconium oxo-clusters and framework decomposition [39]. Quantitative analysis (MP-AES) of the UiO-66-NH_2 represented that the composition of zirconium was 25.1 % of the MOF.

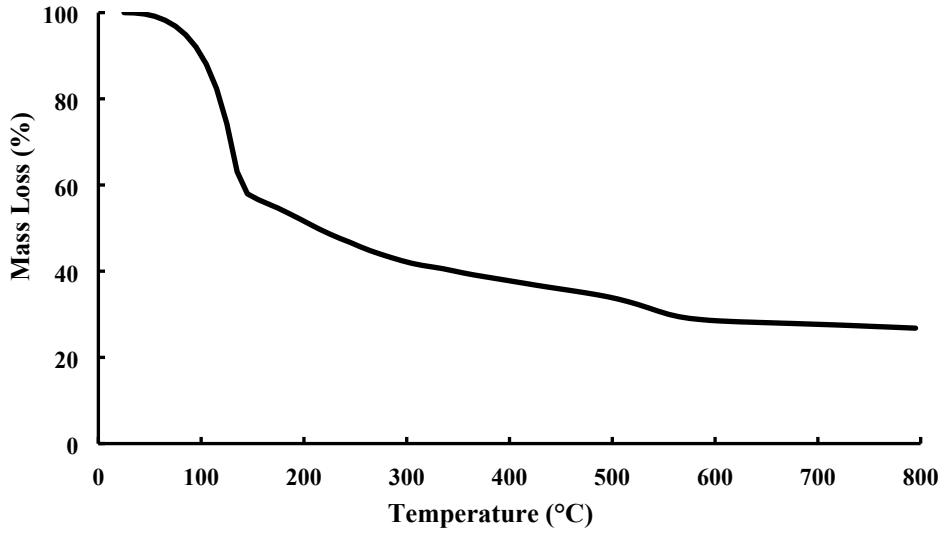

Figure 5. TGA curves of pristine UiO-66-NH_2 (N_2 atmosphere, heating rate 10 ˚C/min).

3.2. Statistical analysis

The experiments were conducted under the specified experimental conditions based on CCD model. The consequences of key factors including reaction temperature, oxidant to sulfur mass ratio, and catalyst to sulfur mass ratio, were studied at the designated reaction time. The values of independent factors, together with predicted and observed responses were given in Table 2. By applying multiple regression analysis on the experimental data, a second-order polynomial equation with coded factors was obtained as shown in Equation 3:

$$\text{DBT Removal (wt\%)} = -25.99 + 2.56 * (X1) + 11.13 * (X2) + 2.30 * (X3) - 0.09 * (X1 * (X2) + 0.006 * (X1) * (X3) - 0.25 * (X2) * (X3) - 0.017 * (X1)2 - 0.52 * (X2)2 - 0.10 * (X3)2 \quad (4)$$

Table 2 Arrangement of CCD and the corresponding measured and predicted results

Run No.	Point type	X1 (°C)	X2 (mg / mg)	X3 (mg / mg)	Removal efficiency (%) Predicted	Experimental
1	Center	60.00	3.25	7.75	87.41	89.02
2	Axial	36.22	4.89	3.44	73.44	73.14
3	Axial	83.78	4.89	12.06	77.97	77.81
4	Factorial	60.00	0.50	7.75	82.62	78.86
5	Axial	83.78	1.61	12.06	87.58	92.63
6	Factorial	100.00	3.25	7.75	70.29	67.60
7	Axial	83.78	1.61	3.44	79.83	79.31
8	Factorial	60.00	3.25	0.50	79.80	77.27
9	Center	60.00	3.25	7.75	87.41	85.18
10	Axial	36.22	4.89	12.06	71.74	77.03
11	Factorial	60.00	6.00	7.75	84.40	81.43
12	Axial	36.22	1.61	3.44	61.71	66.62
13	Axial	83.78	4.89	3.44	77.24	81.26
14	Center	60.00	3.25	7.75	87.41	89.18
15	Factorial	20.00	3.25	7.75	49.81	45.77
16	Factorial	60.00	3.25	15.00	84.89	80.70
17	Axial	36.22	1.61	12.06	67.03	67.77

The analysis of variance (ANOVA) was performed for the fitted quadratic polynomial model of DBT removal (Table 3). The fitness of the quadratic model was evaluated by the coefficient of determination (R^2), and its statistical significance was investigated by Fisher's F-test. Model terms were checked by the p-value (probability) with more than 99% confidence level. From the coded coefficient value for each factor, the temperature has the greatest impact on the DBT removal, after that catalyst dosage and finally oxidant amount in the investigated range. The F-value of 7.79 along with the p-value 0.0065, indicated a high significance of the model (Equation 3). The model F-value of 12.76 also implies that there is only a 0.14% chance that such a large F-value could occur due to noise. Furthermore, the coefficient of determination (R^2 = 0.92) indicated that the predicted mathematical model was well fitted to the experimental data.

Table 3: ANOVA results for the quadratic model of DBT removal efficiency

Source	Sum of Squares	Degree of Freedom	Mean Square	F -Value	p-value Prob > F
A: Temperature (°C)	506.24	1	506.24	20.16	0.0028
B: O/S (mg/mg)	3.84	1	3.84	0.1527	0.7076
C: C/S (mg/mg)	31.27	1	31.27	1.25	0.3013

Source	Sum of Squares	Degree of Freedom	Mean Square	F -Value	p-value Prob > F
AB	102.53	1	102.53	4.08	0.0831
AC	2.92	1	2.92	0.1162	0.7432
BC	24.64	1	24.64	0.9809	0.3550
A^2	1054.84	1	1054.84	42.00	0.0003
B^2	21.46	1	21.46	0.8543	0.3861
C^2	36.09	1	36.09	1.44	0.2696
Model	1760.22	9	195.58	7.79	0.0065
Error	10.26	2	5.13		
R^2 = 91.37 %, Adjusted R^2 = 89.27 %					

The comparison between experimental and predicted values was illustrated in Figure 6, the plot showed the reliability of the model which implied that DBT removal correlation had high accuracy within the investigated range of variables (Equation 3).

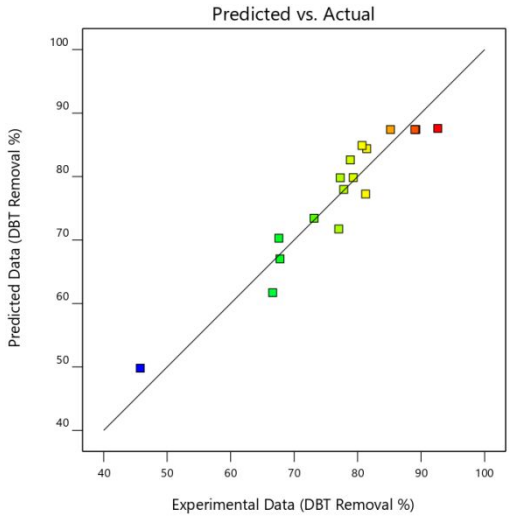

Figure 6. Comparison between experimental and predicted DBT removal yield

Also, Figure 7 depicted the normal % probability plot of the residuals. The normal % probability plot designated whether the residuals show a normal distribution, in which case the points should fall approximately on a straight line. As shown in Figure 7, the reliability of the predicted model was confirmed by the graphical plot.

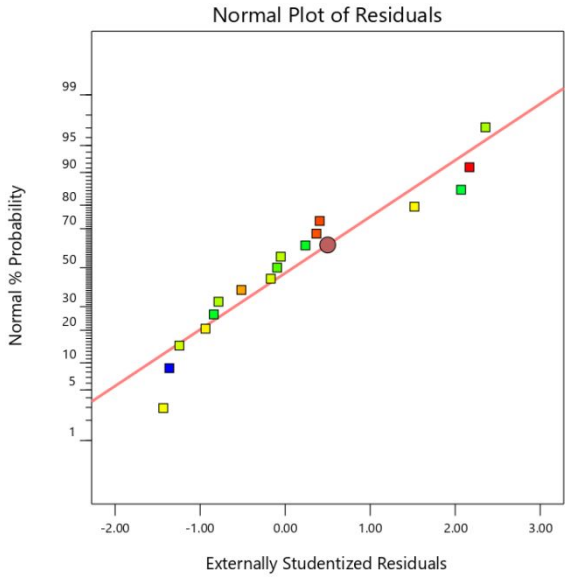

Fig. 7. The plot of normal % probability vs. internally studentized residuals

This research was conducted to determine the influence of individual process variables as well as their interactions by using the benefit of the Design of Experiment (DOE). The significance of each of the three independent parameters (Temperature, O/S mass ratio and C/S mass ratio) on DBT removal efficiency was specified by indicating the response surfaces contours and three-dimensional (3D) plots (Figure 8 and Figure 9). Figure 8 illustrated response surface plots between oxidation temperature reaction and O/S mass ratio on the desulfurization of DBT, which demonstrated that both factors have noticeable effects on removal efficiency and the proper reaction conditions pertinent to the increment of ODS reaction rate. It can be obvious that at a certain temperature, as O/S molar ratio increases up to 1.7, the DBT removal rate first increases and then reduced by further increasing O/S to 8 and more. However, the DBT sulfur removal efficiency grew in the presence of higher amounts of oxidants [40-41], an excess hydrogen peroxide can cause H_2O molecules to occupy the active sites, causing reduced adsorption of DBT on the surface area of MOF. In addition, economic factors to minimize the use of oxidants should be always regarded. Thus, the model calculated the optimal amount of O/S = 1.62 (mg/mg) for ODS reaction.

Also, increasing the temperature from 60 to 72 °C causes growing the DBT removal to a certain O/S, but further increasing the temperature over 72 °C diminished the DBT removal rate. The the desulfurization process is endothermic [42], therefore increasing the temperature leads to increasing ODS reaction rate, also the higher temperature enhances the movement of molecules and thus increases the possibility of collisions between reactants. On the other hand, the increase of temperature contributes to the decomposition of oxidant whereby the concentration of oxidant in the reaction drops and subsequently desulfurization declines [43]. Thus, the optimal temperature can be considered 72 °C.

Figure 9 demonstrated the binary interaction of the reaction temperature and C/S ratio. Obviously, at the C/S ratio of 0.5 to 12 and temperature of 60 to 72 °C, the highest DBT removal was acquired which relates to almost complete oxidation, showing that 12 of the C/S ratio increased the concentration of catalytic active sites at a proper level which led to higher removal efficiency of DBT. However, excessive catalyst dosage tends to cause agglomeration, restrict the contact area with sulfur components, and affect the diffusion of reactants and products, thus the efficiency of catalytic activity in ODS reaction is diminished [44].

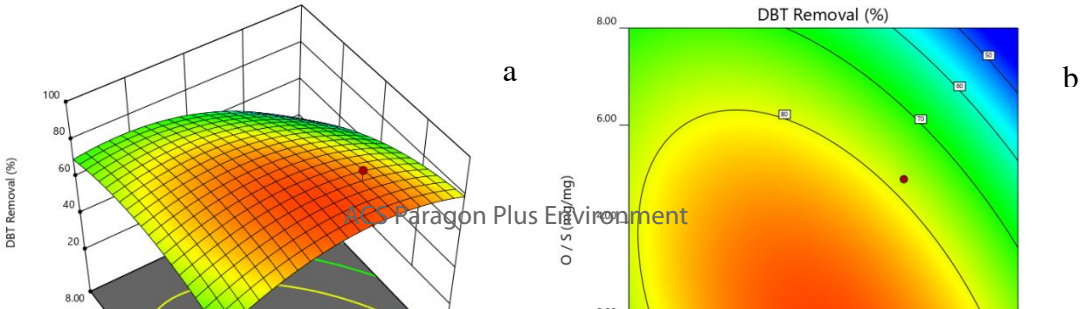

Fig. 8. 3D plot (a) and contour lines (b) presenting the effect of temperature and O/S mass ratio on the removal of DBT from the FM, X3= 12 mg cat. mg^{-1} sulfur.

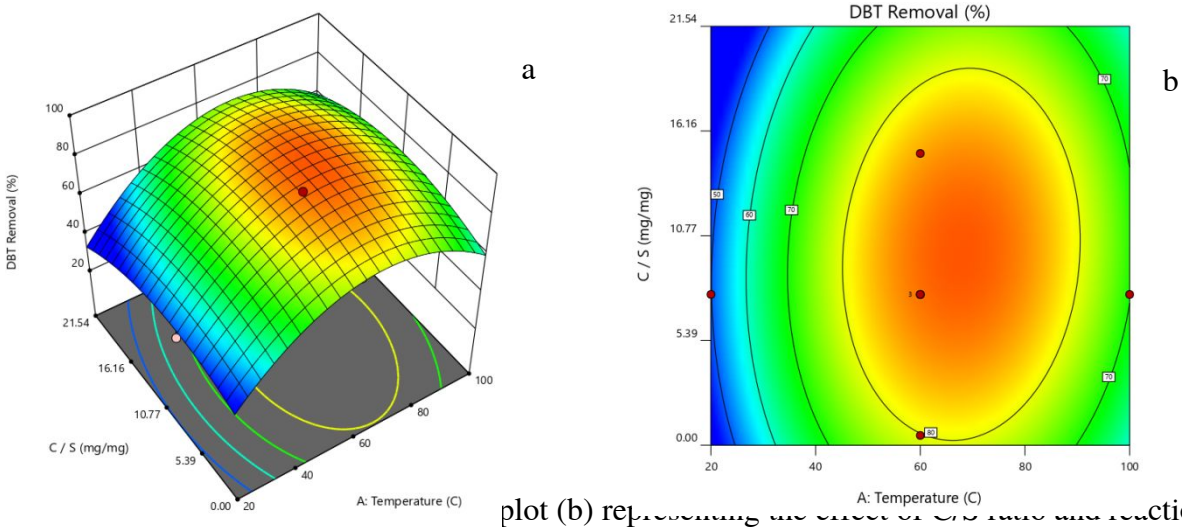

Fig. 8. 3D plot (a) and contour plot (b) representing the effect of O/S ratio and reaction temperature for DBT desulfurization, X2= 1.6 mg Oxidant/mg Sulfur.

3.3. Optimization

The response optimization technique has been evaluated to ascertain the optimal conditions of UiO-66-NH_2 catalyst preparation for ODS process in DBT fuel model. Table 4 displayed the

optimal condition, the predicted and experimental sulfur removal. The optimum values of the three independent variables (Temperature, O/S ratio and C/S) were calculated.

Table 4: Result of confirmation experiments for optimum condition.

Parameter	Optimum Value	DBT Removal (%) Desirability
Temperature (˚C)	72.6	93.8%
O / S ratio (-)	1.62	
C / S ratio (-)	11.03	

3.4. Proposed Mechanism

Figure 10 showed the proposed UiO-66-NH_2 reaction mechanism for DBT catalytic oxidation. Metal cluster units of UiO-66-NH_2 structure connected to 12 rings of amino terephthalic acid, which made it a Lewis-acid-containing catalyst. Accordingly, the MOF was able to strengthen the electrophilicity property of the oxidant with a high electron-withdrawing ability and partially reduced $Zr^{\delta+}$ sites. The oxidative reaction was initiated by the free electrons nucleophilic attack from oxygen species and then reacting with adsorbed DBT molecules to produce sulfoxide [17]. In the following, the sulfoxide was further oxidized to sulfone and then the polar sulfones from the catalysts were desorbed and extracted into the aqueous phase. ODS reaction can occur

without catalyst with less removal efficiency. The benefit of the MOF as a proper catalyst is not only due to high activation of H-O-O-H bonds through forming active oxygen species, but also MOF mechanical stability for reusing in ODS reaction results in higher sulfur removal efficiency [45-46].

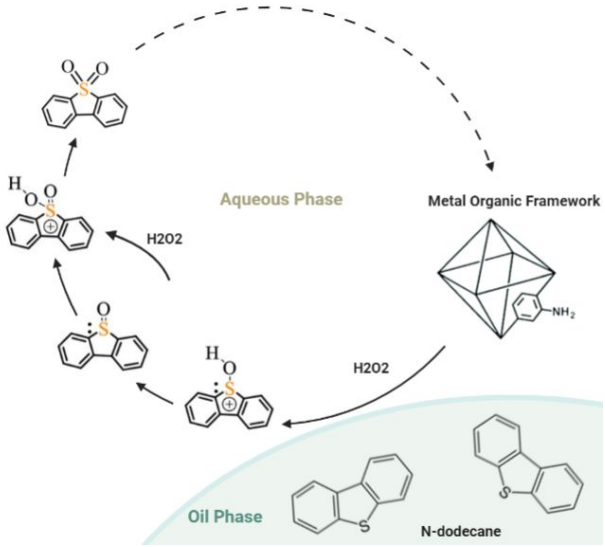

Fig. 10. The proposed mechanism for DBT ODS reaction using UiO-66-NH_2 as catalyst, H_2O_2 as oxidant

3.5. Reusability of Spent Catalyst

The reusability of the catalyst is a property in terms of practical application to economical evaluation. Regeneration of UiO-66-NH_2 MOF catalysts was appraised by carrying out three multiple DBT removal experiments at 70 and 80 °C around the optimal condition. After each

experiment, the MOF was separated from the oil phase and recovered by centrifuge. For eliminating the remain of sulfur it was washed with acetonitrile several times, then drying at 100 °C for 12 hours in an oven and after that reused in the next DBT removal experiment. Figure 11 illustrated that sulfur removal efficiency remained almost the same level with a small decrease trend after four sequential cycles. The gradual drop in the MOF performance for the fifth cycle might be related to a reduction in the availability of active sites in the MOF pores. The sulfone and sulfoxide formed during the catalytic oxidative reaction may be the cause of catalyst deactivation through π-complexation, which cannot be simply removed by washing and heat during the regeneration steps [47].

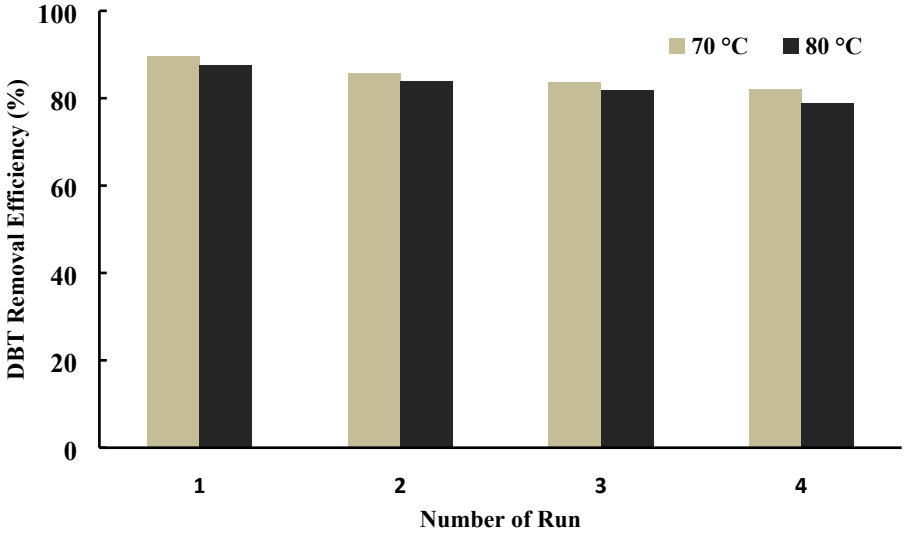

Fig. 11. The effect of UiO-66-NH_2 catalyst recycling (1–4 runs) on DBT removal efficiency

(Condition: 6 ml of model fuel, 15 mg MOF, O/ S = 1.6, 6 ml of acetonitrile, 150 min, at 70 / 80 °C).

4. Conclusion

Functionalized UiO-66(Zr) was successfully synthesized by ligand substitution through a solvothermal methodology. The structure of MOF catalysts was confirmed by various characterization. The effect of several parameters on the oxidative catalytic desulfurization efficiency was studied in detail, including temperature, O/S mass ratio and C/S mass ratio using RSM-CCD technique. According to the values of the model fitness parameters, the experimental results were acceptable adapted to the predicted data with an appropriate R^2. The removal efficiency of sulfur could reach 93.8%, in 72.6 ◦C, O/S ratio: 1.62, and C/S ratio: 11.03 for DBT FM (1000 ppm S content). Furthermore, the results of repeated use demonstrated that the employed MOF has acceptable recyclability and maintains its catalytic performance up to four cycles with little drop.

5. Acknowledgment

The authors appreciate the supports of Faculty of Engineering, Virumaa College of Tallinn University of Technology and thankful to Stat-Ease, Minneapolis, MN, USA, for providing the Design-Expert 12 Package.

6. Reference

[1] Huang, Chongpin, et al. "Desulfurization of gasoline by extraction with new ionic liquids." *Energy & Fuels* 18.6 (2004): 1862-1864.

[2] Toutov, Anton A., et al. "A potassium tert-butoxide and hydrosilane system for ultra-deep desulfurization of fuels." *Nature Energy* 2.3 (2017): 1-7.

[3] Li, Shuai-Shuai, et al. "Controllable fabrication of cuprous sites in confined spaces for efficient adsorptive desulfurization." *Fuel* 259 (2020): 116221.

[4] Muhammad, Yaseen, et al. "Boosting the hydrodesulfurization of dibenzothiophene efficiency of Mn decorated (Co/Ni)-Mo/Al_2O_3 catalysts at mild temperature and pressure by coupling with phosphonium based ionic liquids." *Chemical Engineering Journal* 375 (2019): 121957.

[5] Shafiq, Iqrash, et al. "Recent developments in alumina supported hydrodesulfurization catalysts for the production of sulfur-free refinery products: A technical review." *Catalysis Reviews* (2020): 1-86.

[6] Liu, Yaqing, et al. "Ultra-deep desulfurization by reactive adsorption desulfurization on copper-based catalysts." *Journal of Energy Chemistry* 29 (2019): 8-16.

[7] Rajendran, Antony, et al. "A comprehensive review on oxidative desulfurization catalysts targeting clean energy and environment." *Journal of Materials Chemistry A* 8.5 (2020): 2246-2285.

[8] Andevary, Hojatollah Haji, Azam Akbari, and Mohammadreza Omidkhah. "High efficient and selective oxidative desulfurization of diesel fuel using dual-function [Omim] $FeCl_4$ as catalyst/extractant." *Fuel Processing Technology* 185 (2019): 8-17.

[9] Gu, Qingqing, et al. "Reduced graphene oxide: a metal-free catalyst for aerobic oxidative desulfurization." *Green Chemistry* 19.4 (2017): 1175-1181.

[10] Wang, Danhong, et al. "Oxidative desulfurization of fuel oil: Part I. Oxidation of dibenzothiophenes using tert-butyl hydroperoxide." *Applied Catalysis A: General* 253.1 (2003): 91-99.

[11] Jiang, Zongxuan, et al. "Oxidative desulfurization of fuel oils." *Chinese journal of catalysis* 32.5 (2011): 707-715.

[12] Bhadra, Biswa Nath, and Sung Hwa Jhung. "Oxidative desulfurization and denitrogenation of fuels using metal-organic framework-based/-derived catalysts." *Applied Catalysis B: Environmental* 259 (2019): 118021.

[13] Howarth, Ashlee J., et al. "Best practices for the synthesis, activation, and characterization of metal–organic frameworks." *Chemistry of Materials* 29.1 (2017): 26-39.

[14] Smolders, Simon, et al. "A Titanium (IV)-Based Metal–Organic Framework Featuring Defect-Rich Ti-O Sheets as an Oxidative Desulfurization Catalyst." *Angewandte Chemie* 131.27 (2019): 9258-9263.

[15] Gascon, Jorge, et al. "Metal organic framework catalysis: quo vadis?." *Acs Catalysis* 4.2 (2014): 361-378.

[16] Ye, Gan, et al. "Enhancement of oxidative desulfurization performance over UiO-66 (Zr) by titanium ion exchange." *ChemPhysChem* 18.14 (2017): 1903-1908.

[17] Zhang, Xiaotian, et al. "A metal–organic framework for oxidative desulfurization: UIO-66 (Zr) as a catalyst." *Fuel* 209 (2017): 417-423.

[18] Viana, Alexandre M., et al. "Influence of UiO-66 (Zr) preparation strategies in its catalytic efficiency for desulfurization process." *Materials* 12.18 (2019): 3009.

[19] Zhang, Xiong-Fei, et al. "Adsorptive desulfurization from the model fuels by functionalized UiO-66 (Zr)." *Fuel* 234 (2018): 256-262.

[20] Liao, Xiaoyuan, et al. "Ligand Modified Metal Organic Framework UiO-66: A Highly Efficient and Stable Catalyst for Oxidative Desulfurization." *Journal of Inorganic and Organometallic Polymers and Materials* 31.2 (2021): 756-762.

[21] Li, Zhi, et al. "Capture of H2S and SO2 from trace sulfur containing gas mixture by functionalized UiO-66 (Zr) materials: A molecular simulation study." *Fluid Phase Equilibria* 427 (2016): 259-267.

[22] Ye, Gan, et al. "Green and scalable synthesis of nitro-and amino-functionalized UiO-66 (Zr) and the effect of functional groups on the oxidative desulfurization performance." *Inorganic Chemistry Frontiers* 6.5 (2019): 1267-1274.

[23] Luu, Cam Loc, et al. "Synthesis, characterization and adsorption ability of UiO-66-NH2." *Advances in Natural Sciences: Nanoscience and Nanotechnology* 6.2 (2015): 025004.

[24] Peterson, Gregory W., et al. "Extraordinary NO2 Removal by the Metal–Organic Framework UiO-66-NH2." *Angewandte Chemie* 128.21 (2016): 6343-6346.

[25] Zhang, Jinhui, et al. "TiO2-UiO-66-NH2 nanocomposites as efficient photocatalysts for the oxidation of VOCs." *Chemical Engineering Journal* 385 (2020): 123814.

[26] Jiang, Xue, et al. "Deep desulfurization of fuels catalyzed by surfactant-type decatungstates using H2O2 as oxidant." *Fuel* 88.3 (2009): 431-436.

[27] García-Gutiérrez, José Luis, et al. "Ultra-deep oxidative desulfurization of diesel fuel with H2O2 catalyzed under mild conditions by polymolybdates supported on Al_2O_3." *Applied Catalysis A: General* 305.1 (2006): 15-20.

[28] Jiang, Xue, et al. "Deep desulfurization of fuels catalyzed by surfactant-type decatungstates using H2O2 as oxidant." *Fuel* 88.3 (2009): 431-436.

[29] Zheng, He-Qi, et al. "Zr-based metal–organic frameworks with intrinsic peroxidase-like activity for ultradeep oxidative desulfurization: mechanism of H_2O_2 decomposition." *Inorganic chemistry* 58.10 (2019): 6983-6992.

[30] Katz, Michael J., et al. "A facile synthesis of UiO-66, UiO-67 and their derivatives." *Chemical Communications* 49.82 (2013): 9449-9451.

[31] Barghi, Bijan, Allan Niidu, and Ramin Karimzadeh. "The effect of water and zinc loading on LPG catalytic cracking for light olefin production using Response Surface Methodology." *Proceedings of the Estonian Academy of Sciences* 70.2 (2021).

[32] Bezerra, Marcos Almeida, et al. "Response surface methodology (RSM) as a tool for optimization in analytical chemistry." *Talanta* 76.5 (2008): 965-977.

[33] Zlotea, Claudia, et al. "Effect of NH_2 and CF_3 functionalization on the hydrogen sorption properties of MOFs." *Dalton Transactions* 40.18 (2011): 4879-4881.

[34] Kim, Min, et al. "Postsynthetic modification at orthogonal reactive sites on mixed, bifunctional metal–organic frameworks." *Chemical Communications* 47.27 (2011): 7629-7631.

[35] Vermoortele, Frederik, et al. "An amino-modified Zr-terephthalate metal–organic framework as an acid–base catalyst for cross-aldol condensation." *Chemical communications* 47.5 (2011): 1521-1523.

[36] Vermoortele, Frederik, et al. "Electronic effects of linker substitution on Lewis acid catalysis with metal–organic frameworks." *Angewandte Chemie International Edition* 51.20 (2012): 4887-4890.

[37] Shearer, Greig C., et al. "In situ infrared spectroscopic and gravimetric characterisation of the solvent removal and dehydroxylation of the metal organic frameworks UiO-66 and UiO-67." *Topics in Catalysis* 56.9-10 (2013): 770-782.

[38] Zhu, Junjie, et al. "Polyethyleneimine-modified UiO-66-NH_2 (Zr) metal–organic frameworks: preparation and enhanced CO2 selective adsorption." *ACS omega* 4.2 (2019): 3188-3197.

[39] Fang, Yunxia, et al. "Application of acid-promoted UiO-66-NH_2 MOFs in the treatment of wastewater containing methylene blue." *Chemical Papers* 73.6 (2019): 1401-1411.

[40] Saleh, Tawfik A. "Simultaneous adsorptive desulfurization of diesel fuel over bimetallic nanoparticles loaded on activated carbon." *Journal of Cleaner Production* 172 (2018): 2123-2132.

[41] Fox, Brandy R., et al. "Enhanced oxidative desulfurization in a film-shear reactor." *Fuel* 156 (2015): 142-147.

[42] Abbaslou, Reza M. Malek, et al. "Iron catalysts supported on carbon nanotubes for Fischer–Tropsch synthesis: Effect of catalytic site position." *Applied Catalysis A: General* 367.1-2 (2009): 47-52.

[43] Akbari, Azam, Mohammadreza Omidkhah, and Darian Jafar Towfighi. "Optimization of operating conditions in oxidation of dibenzothiophene in the light hydrocarbon model." *Chemical Industry and Chemical Engineering Quarterly* 20.3 (2014): 315-323.

[44] Cao, Ying, et al. "Highly efficient oxidative desulfurization of dibenzothiophene using Ni modified MoO_3 catalyst." *Applied Catalysis A: General* 589 (2020): 117308.

[45] Di Giuseppe, Andrea, et al. "Efficient oxidation of thiophene derivatives with homogeneous and heterogeneous MTO/H2O2 systems: a novel approach for, oxidative desulfurization (ODS) of diesel fuel." *Applied Catalysis B: Environmental* 89.1-2 (2009): 239-245.

[46] Wei, Sainan, et al. "Performances, kinetics and mechanisms of catalytic oxidative desulfurization from oils." *RSC advances* 6.105 (2016): 103253-103269.

[47] Ren, Xiaoling, et al. "Dynamic catalytic adsorptive desulfurization of real diesel over ultra-stable and low-cost silica gel-supported TiO_2." *AIChE Journal* 64.6 (2018): 2146-2159.